

## Fine and Hyperfine Structure of the $2^2P$ Term of $\text{Li}^6$ and $\text{Li}^7$ †

K. C. BROG,\* T. G. ECK, AND H. WIEDER‡

*Physics Department, Case Institute of Technology, Cleveland, Ohio*

(Received 26 August 1966)

Interference signals in resonance fluorescence associated with the crossing of the  $J = \frac{3}{2}$ ,  $m_J = -\frac{3}{2}$  and  $J = \frac{1}{2}$ ,  $m_J = \frac{1}{2}$  fine-structure Zeeman levels were used to investigate the fine and hyperfine structure of the  $2^2P$  term of  $\text{Li}^6$  and  $\text{Li}^7$ . The magnetic field strength corresponding to this crossing was determined for each isotope to within 1 part in  $4.5 \times 10^4$ . However, the precision with which the fine-structure splitting can be inferred from the crossing field is limited at the present time by a lack of knowledge of relativistic and diamagnetic corrections to the orbital  $g$  factor  $g_L$ . The  $\text{Li}^7$  signal exhibited well-resolved hyperfine structure. Measurements of this structure have been used together with Ritter's result for the hyperfine splitting in the  $2^2P_{1/2}$  state to obtain values for  $a_{c,3/2}$  and  $a_{d,3/2}$ , the Fermi contact and dipole-dipole contributions to the magnetic hyperfine interaction in the  $2^2P_{3/2}$  state of  $\text{Li}^7$ , and a value for  $Q$ , the quadrupole moment of the  $\text{Li}^7$  nucleus. They are:  $a_{c3/2} = -10.53 \pm 0.23$  Mc/sec,  $a_{d3/2} = 7.13 \pm 0.03$  Mc/sec, and  $Q = (-3 \pm 2) \times 10^{-26}$  cm<sup>2</sup>. The widths of the hyperfine components of the  $\text{Li}^7$  crossing signal yield  $(2.72 \pm 0.04) \times 10^{-8}$  sec for the lifetime of the  $2^2P$  term of atomic lithium.

### I. INTRODUCTION

THE level-crossing technique of atomic spectroscopy developed by Colegrove, Franken, Lewis, and Sands<sup>1</sup> utilizes an interference effect in resonance fluorescence which can occur when two Zeeman levels arising from different fine- or hyperfine-structure levels are tuned to the same energy ("crossed") by the application of an external magnetic field. We have used this technique to investigate the fine and hyperfine structure of the  $2^2P$  term of atomic lithium. The initial motivation for undertaking this study was to obtain a precise value for the fine-structure splitting in the  $2^2P$  term of lithium which, in principle, could be used for a redetermination of the fine structure constant  $\alpha$ . Dayhoff, Triebwasser, and Lamb<sup>2</sup> determined  $\alpha$  from a measurement of the fine-structure splitting in the  $2^2P$  term of deuterium. The precision of this measurement (2 parts in  $10^5$ ) is limited by the rather broad radiation width (100 Mc/sec) of the levels of this term associated with a  $1.6 \times 10^{-9}$  sec lifetime. The  $2^2P$  term of lithium, with a lifetime of  $2.7 \times 10^{-8}$  sec and a fine-structure splitting comparable to that of deuterium, would seem to offer the possibility of obtaining a more precise value of  $\alpha$ , although the theoretical difficulties to be encountered in relating the fine-structure splitting to  $\alpha$  are all too obvious.

Goodings<sup>3</sup> has calculated the magnetic-dipole hyperfine-interaction constants for the  $2^2P$  term of  $\text{Li}^7$  using the unrestricted Hartree-Fock (UHF) approximation to treat the exchange polarization of the  $1s$  core electrons by the  $2p$  valence electron. There has been much discussion in the literature of the past several years

concerning the adequacy of the UHF approach for treatment of magnetic hyperfine interactions in atomic systems in general and in lithium in particular.<sup>4</sup> Although the majority opinion seems to be that the UHF predictions should be quite accurate for the  $2^2P$  terms of lithium, there have not been until recently any experimental values to compare with these theoretical predictions. Ritter's<sup>5</sup> optical double resonance measurements give  $46.17 \pm 0.35$  Mc/sec for the magnetic dipole interaction constant in the  $2^2P_{1/2}$  state of  $\text{Li}^7$ , which is to be compared with Goodings's calculated value of 43.1 Mc/sec. Although this agreement is quite good when one considers that Goodings's calculation did not take into account the effect of correlation on the wave function of the  $p$  electron, it is not possible using Ritter's result alone to separate out the contribution to the magnetic hyperfine interaction arising from the polarized core from that due to the valence electron. Thus, it is not certain that the discrepancy between Goodings's and Ritter's values is due solely to Goodings's neglect of correlation effects.

In the present paper we use the form of the UHF approach to analyze our hyperfine-structure data. By combining our results with that of Ritter we have been able not only to evaluate separately the contributions arising from the polarized core and the valence electron, but have also been able to obtain a check on the consistency of our treatment of the hyperfine interaction which is independent of any detailed knowledge of the electronic wave function.

Figure 1 shows the dependence on magnetic field strength of the energy of the fine-structure levels of a  $2^2P$  term. There are two level crossings, the crossing of the  $J = \frac{3}{2}$ ,  $m_J = -\frac{3}{2}$  and  $J = \frac{1}{2}$ ,  $m_J = \frac{1}{2}$  levels and the crossing of the  $\frac{3}{2}$ ,  $-\frac{3}{2}$  and  $\frac{1}{2}$ ,  $-\frac{1}{2}$  levels. We shall refer to these two crossings as the low- and high-field crossing, respectively. For the  $2^2P$  term of Li they occur at

† Work supported by the National Science Foundation.

\* Present address: Physics of Solids Division, Battelle Memorial Institute, Columbus, Ohio.

‡ Present address: IBM T. J. Watson Research Center, Yorktown Heights, New York.

<sup>1</sup> F. D. Colegrove, P. A. Franken, R. R. Lewis, and R. H. Sands, *Phys. Rev. Letters* **3**, 420 (1959).

<sup>2</sup> E. S. Dayhoff, S. Triebwasser, and W. E. Lamb, Jr., *Phys. Rev.* **89**, 106 (1953).

<sup>3</sup> D. A. Goodings, *Phys. Rev.* **123**, 1706 (1961).

<sup>4</sup> E. A. Burke, *Phys. Rev.* **135**, A621 (1964) and references contained therein.

<sup>5</sup> G. J. Ritter, *Can. J. Phys.* **40**, 770 (1965).

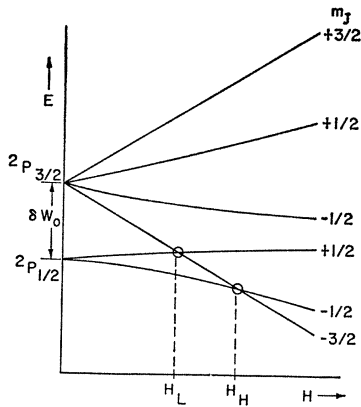


FIG. 1. Variation with magnetic field strength of the energies of the fine-structure Zeeman levels of a  $2P$  term.

field strengths of approximately 3200 and 4800 G. Each of the fine-structure crossings of Fig. 1 is actually an array of many crossings, since each  $m_J$  level is split into  $2I+1$  levels both by the hyperfine interaction between the electrons and the nucleus with spin  $I$  and the Zeeman interaction between the nucleus and the external magnetic field. Figure 2 shows the eight levels of the low-field crossing in  $\text{Li}^7$  ( $I = \frac{3}{2}$ ). The corresponding figure for the high-field crossing is much more complicated, since in the vicinity of the high-field crossing eigenstates of the same  $m_F = m_I + m_J$  are strongly coupled by the magnetic hyperfine interaction. This coupling of states leads not only to a distortion of the normal level-crossing signal, but to the presence of added signals associated with what we have termed the "anticrossing" of energy levels.<sup>6</sup> The phenomenon of anticrossing and the treatment of the high-field crossing data are discussed in detail in the following paper. In the present paper we shall consider only the data obtained from the low-field crossing.

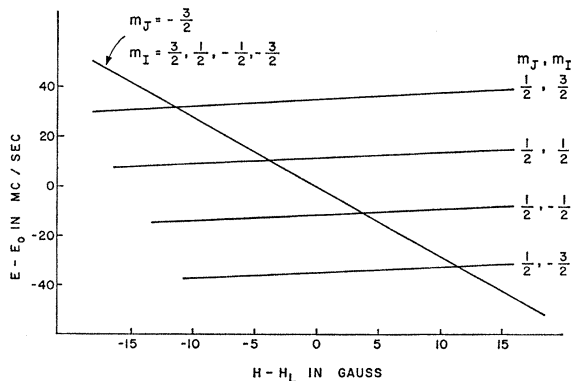


FIG. 2. The eight hyperfine levels involved in the low-field fine-structure crossing in the  $2^2P$  term of  $\text{Li}^7$ . At this magnetic field strength ( $H_L \approx 3200$  G) the spacing of the four  $m_I$  levels with  $m_J = -\frac{3}{2}$  is less than 1% of the spacing of the four  $m_I$  levels with  $m_J = +\frac{1}{2}$ .

<sup>6</sup> T. G. Eck, L. L. Foldy, and H. Wieder, Phys. Rev. Letters 10, 239 (1963).

## II. THEORY

### A. Fine Structure

The fine structure and electronic Zeeman parts of the atomic Hamiltonian are

$$\mathcal{H}_{fs} = A\mathbf{L} \cdot \mathbf{S} + g_L \mu_0 \mathbf{L} \cdot \mathbf{H} + g_S \mu_0 \mathbf{S} \cdot \mathbf{H}. \quad (1)$$

The diagonalization of  $\mathcal{H}_{fs}$  is straightforward for a doublet term, and expressions for the resultant energy levels and eigenfunctions are given in numerous spectroscopy texts.<sup>7</sup> The magnetic field strengths corresponding to the low- and high-field crossings are obtained by equating the expressions for the energies of the relevant levels. This procedure gives

$$\mu_0 H_L / A = (g_S + 2g_L) / 2g_L (g_S + g_L), \quad (2a)$$

$$\mu_0 H_H / A = (g_S + 2g_L) / 2g_L g_S. \quad (2b)$$

The fine structure separation  $\delta W_0 = \frac{3}{2} A$  can be calculated from a determination of either  $\mu_0 H_L$  or  $\mu_0 H_H$ .

### B. Hyperfine Structure

The hyperfine structure and nuclear Zeeman parts of the atomic Hamiltonian are

$$\mathcal{H}_{hfs} = \mathcal{H}_D + \mathcal{H}_Q - g_I \mu_0 \mathbf{I} \cdot \mathbf{H}. \quad (3)$$

The first two terms refer to the magnetic dipole and electric quadrupole parts of the hyperfine interaction, respectively, and the last term gives the interaction between the magnetic moment of the nucleus and the applied magnetic field. With the usual assumption that  $\mathcal{H}_D$  can be written as the sum of single-particle operators, we have

$$\mathcal{H}_D = \alpha \sum_i \left[ \frac{\mathbf{1}_i - \mathbf{s}_i}{r_i^3} + 3 \frac{(\mathbf{s}_i \cdot \mathbf{r}_i) \mathbf{r}_i}{r_i^5} \right] \cdot \mathbf{I} + \beta \sum_i [\mathbf{s}_i \delta(\mathbf{r}_i)] \cdot \mathbf{I}, \quad (4)$$

where  $\alpha = 2\mu_I \mu_0 / I$ ,  $\beta = (16\pi/3)\mu_I \mu_0 / I$ , and  $\delta(\mathbf{r}_i)$  is the Dirac delta function. The first term of Eq. (4) is the dipole-dipole interaction, the matrix elements of which vanish for  $s$  electrons, while the second term is the Fermi contact interaction, which is zero except for  $s$  electrons.

We shall now show that to the extent that one can use a UHF approach to the  $2^2P$  term of  $\text{Li}$  it is possible to transform Eq. (4) so that the matrix elements of  $\mathcal{H}_D$  can be expressed quite simply in terms of only two undetermined constants. These correspond to Goodings's<sup>8</sup>  $a_{c3/2}$ , the Fermi contact interaction constant in the  $P_{3/2}$  state, and  $a_{d3/2}$ , the dipole-dipole interaction constant in the  $P_{3/2}$  state. The corresponding interaction constants in the  $P_{1/2}$  state are  $a_{c1/2} = -a_{c3/2}$  and  $a_{d1/2} = 5\theta a_{d3/2}$ , where  $\theta$  is a relativistic correction factor, which for  $\text{Li}$  is equal to 1 to within a part in  $10^3$ . Goodings's formalism cannot be taken over intact, since it is tailored for low magnetic fields where  $J$  is a good

<sup>7</sup> See, for example, H. G. Kuhn, *Atomic Spectra* (Academic Press Inc., New York, 1962).

quantum number, while our measurements were made at intermediate fields where there is substantial decoupling of  $\mathbf{L}$  and  $\mathbf{S}$ . We take the electronic wave function to be a Slater determinant formed from the product wave function  $\psi_{1s\uparrow}(1)\psi_{1s\downarrow}(2)\psi_{2p\uparrow}(3)$ , where the orbital associated with  $\psi_{1s\uparrow}$  is allowed to differ from that associated with  $\psi_{1s\downarrow}$ . The meaning of the subscript notation is the same as that in Goodings's paper, with the arrow indicating the electron's spin state, except for one slight modification. We take  $\psi_{1s\uparrow}$  to refer not necessarily to the 1s electron with  $m_s = +\frac{1}{2}$ , but to the 1s electron whose spin state is the same as that of the 2p electron. Each of the single-particle wave functions in the product wave function is orthogonal to the other two, since the 2p orbital is orthogonal to each of the 1s orbitals and the 1s wave functions are orthogonal to one another via their spin parts. Since the single-particle wave functions are orthogonal to one another and  $\mathcal{H}_D$  is a sum of single-particle operators, the matrix elements of  $\mathcal{H}_D$  calculated using the full determinantal wave function reduce to sums of matrix elements calculated using the single-particle wave functions. Thus, Eq. (4) simplifies to

$$\mathcal{H}_D = \alpha \left[ \frac{\mathbf{I}_3 - \mathbf{s}_3}{r_3^3} + 3 \frac{(\mathbf{s}_3 \cdot \mathbf{r}_3) \mathbf{r}_3}{r_3^5} \right] \cdot \mathbf{I} + \beta [\mathbf{s}_1 |\psi_1(0)|^2 + \mathbf{s}_2 |\psi_2(0)|^2] \cdot \mathbf{I},$$

where the subscript 3 in the dipole-dipole term is now used simply to indicate that this operator is to be evaluated using the 2p wave function and the subscripts 1 and 2 in the Fermi contact term refer to the two 1s electrons. Of course, at this point we have lost any indication as to which of the 1s electrons is to be associated with the s-state wave function corresponding to spin parallel to that of the 2p electron and, indeed, must proceed in a manner which treats each of the 1s electrons on an equal footing. This can be accomplished by replacing  $|\psi_1(0)|^2$  by

$$|\psi_{\uparrow}(0)|^2 (\mathbf{s}_1 \cdot \mathbf{s}_3 + \frac{3}{4}) + |\psi_{\downarrow}(0)|^2 (-\mathbf{s}_1 \cdot \mathbf{s}_3 + \frac{1}{4})$$

and  $|\psi_2(0)|^2$  by the same expression with  $\mathbf{s}_2$  in place of  $\mathbf{s}_1$ . This says that  $\psi_{\uparrow}(0) = \psi_{\uparrow}(0)$  if  $\mathbf{s}_1$  is parallel to  $\mathbf{s}_3$  (3 referring to the 2p electron) and  $\psi_{\downarrow}(0) = \psi_{\downarrow}(0)$  if  $\mathbf{s}_1$  is antiparallel to  $\mathbf{s}_3$ . Making these substitutions, collecting terms, and using the fact that  $\mathbf{s}_1 + \mathbf{s}_2 = 0$ , we have for the Fermi contact term

$$\beta [(\mathbf{s}_1 \cdot \mathbf{I})(\mathbf{s}_1 \cdot \mathbf{s}_3) + (\mathbf{s}_2 \cdot \mathbf{I})(\mathbf{s}_2 \cdot \mathbf{s}_3)] [|\psi_{\uparrow}(0)|^2 - |\psi_{\downarrow}(0)|^2].$$

This expression can be further simplified using the following property of the spin operator:

$$(\mathbf{s} \cdot \mathbf{a})(\mathbf{s} \cdot \mathbf{b}) = \frac{1}{4}(\mathbf{a} \cdot \mathbf{b}) + \frac{1}{2}i\mathbf{s} \cdot (\mathbf{a} \times \mathbf{b}),$$

where  $\mathbf{a}$  and  $\mathbf{b}$  commute with  $\mathbf{s}$ , but do not necessarily commute with each other. Using this relation and again remembering that  $\mathbf{s}_1 + \mathbf{s}_2 = 0$ , we obtain for the Fermi

contact term

$$\frac{1}{2}\beta [|\psi_{\uparrow}(0)|^2 - |\psi_{\downarrow}(0)|^2] \mathbf{s}_3 \cdot \mathbf{I}.$$

Thus, we have for the final form of  $\mathcal{H}_D$

$$\mathcal{H}_D = \alpha \left[ \frac{\mathbf{I} - \mathbf{s}}{r^3} + 3 \frac{(\mathbf{s} \cdot \mathbf{r}) \mathbf{r}}{r^5} \right] \cdot \mathbf{I} + \xi \mathbf{s} \cdot \mathbf{I}, \quad (5)$$

where  $\xi = (\beta/2)[|\psi_{\uparrow}(0)|^2 - |\psi_{\downarrow}(0)|^2]$  and we have dropped the subscript 3, since all the matrix elements of  $\mathcal{H}_D$  are now to be evaluated using only the wave function of the 2p electron. The matrix elements of  $\mathcal{H}_D$  required for the reduction of the hyperfine structure data are given in Appendix A. They are expressed in terms of the two constants  $\xi$  and  $\alpha \langle 1/r^3 \rangle$ , where  $\langle 1/r^3 \rangle$  refers to an average over the wave function of the 2p electron. Goodings's interaction constants are given in terms of the above constants by

$$a_{c3/2} = \xi/3 \quad (6)$$

$$a_{d3/2} = (8/15)\alpha \langle 1/r^3 \rangle.$$

Thus, within the framework of the UHF approach,  $\xi$  and  $\alpha \langle 1/r^3 \rangle$  characterize, respectively, the core and valence electron contributions to the magnetic hyperfine interaction.

The matrix elements of the electric quadrupole Hamiltonian  $\mathcal{H}_Q$  are given in Appendix B. They are proportional to  $Q \langle 1/r^3 \rangle$ , where  $Q$  is the electric quadrupole moment of the lithium nucleus and  $\langle 1/r^3 \rangle$  is the same average over the 2p electron wave function that appears in the dipole-dipole part of the matrix elements of  $\mathcal{H}_D$ . To the precision of our data, quadrupole contributions to the hyperfine interaction are negligible in  $\text{Li}^6$ , but not in  $\text{Li}^7$ . From our hyperfine structure data, we have obtained a value for  $Q(\text{Li}^7)$  which, while of low precision, is in good agreement with the more precise value determined from the quadrupole coupling constant in  $\text{LiH}$ .<sup>8</sup>

### C. Level-Crossing Signal

Franken<sup>9</sup> and Rose and Carovillano<sup>10</sup> have analyzed in detail the interference effects in resonance fluorescence which occur when Zeeman levels cross and have discussed the magnitude and shape of the interference signal as a function of level separation for various experimental geometries. The signal associated with the crossing of two levels  $a$  and  $b$  is given by

$$S = c \left[ \frac{(B+B^*)\gamma^2}{\gamma^2 + \Delta^2} - \frac{(B-B^*)i\gamma\Delta}{\gamma^2 + \Delta^2} \right], \quad (7)$$

<sup>8</sup> S. L. Kahalas and R. K. Nesbet, Phys. Rev. Letters **6**, 549 (1961) and J. Chem. Phys. **39**, 529 (1963). L. Wharton, L. P. Gold, and W. Klemperer, *ibid.* **37**, 2149 (1962); Phys. Rev. **133**, B270 (1964).

<sup>9</sup> P. A. Franken, Phys. Rev. **121**, 508 (1961).

<sup>10</sup> M. E. Rose and R. L. Carovillano, Phys. Rev. **122**, 1185 (1961).

where  $\Delta$  is the frequency separation of the levels  $a$  and  $b$ ,  $\gamma$  is the radiative width in frequency units of the excited state ( $\gamma = 1/2\pi\tau$ , where  $\tau$  is the mean life of the excited state), and  $c$  is a parameter proportional to the intensity of the incident radiation, geometrical factors, etc. The symbol  $B$  denotes a sum of products of the relevant electric dipole matrix elements, i.e.,

$$B = \sum_{m,m'} f_{am} f_{mb} g_{bm'} g_{m'a}$$

where  $f_{am} = \langle a | \mathbf{f} \cdot \mathbf{r} | m \rangle$  etc. and  $\mathbf{f}$  and  $\mathbf{g}$  refer to the polarizations of the absorbed and re-emitted photons, respectively. The letters  $m$  and  $m'$  label the initial and final states in the resonance fluorescence process.

If  $B$  is real the second term in Eq. (7) vanishes and the signal has a Lorentzian lineshape [see Fig. 3(a) of Ref. 9], while for  $B$  imaginary the first term in Eq. (7) vanishes and the signal has a dispersion-type line shape [see Fig. 3(b) of Ref. 9]. The character of  $B$  depends on the directions and polarizations of the incoming and outgoing light. For ease in interpreting the observed crossing signal, it is obviously advantageous to choose an experimental geometry for which  $B$  is, as nearly as possible, either real or imaginary. Our observations were made with the directions of the incident and scattered light at right angles to that of the magnetic field and at right angles to each other. With this geometry the low-field crossing signal in a  $^2P$  term of Li has a Lorentzian lineshape.

It follows from the above expression for  $B$  that to observe a crossing signal it must be possible to excite both of the crossing levels by an electric dipole transition from the initial state of the atom, i.e.,  $f_{am}$  and  $f_{bm}$  must both be nonzero for at least one  $m$ . At the magnetic field strengths corresponding to the fine-structure crossings in Li, the nuclear angular momentum is well decoupled from the electronic angular momentum and the selection rule  $\Delta m_I = 0$  applies for electric dipole transitions. Thus, only the crossing of levels of the same  $m_I$  can yield a level-crossing signal. Of the sixteen crossings in Fig. 2 only four produce signals.

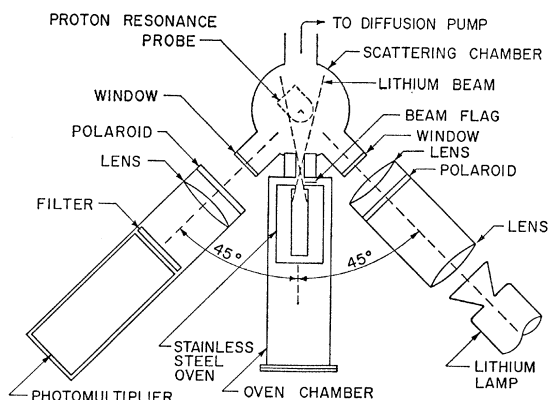


FIG. 3. Schematic diagram of the experimental apparatus.

### III. EXPERIMENTAL DETAILS

The essentials of the apparatus used for this investigation are shown in Fig. 3. Light from a lithium resonance lamp, scattered through an angle of approximately  $90^\circ$  from a dense beam of atomic lithium, was viewed by a photomultiplier tube. The beam was generated by evaporating lithium from a stainless steel oven and passed through a collimating channel into the "scattering" chamber. Interruption of the lithium beam by a "beam flag" allowed that part of the total photomultiplier signal which was due to scattering of light from the walls of the chamber to be determined. The brass vacuum envelope was placed in the  $2\frac{1}{4}$ -inch gap between the pole faces of a 12-in. electromagnet with the scattering volume (volume of intersection of the atomic beam and incident light beam) situated in the most homogeneous region of the magnetic field. The magnetic field strength was measured by a proton resonance probe placed adjacent to the scattering volume, but outside of the vacuum envelope. The polarizations of the incident and detected light were determined by the orientations of HN-32 Polaroid sheets.

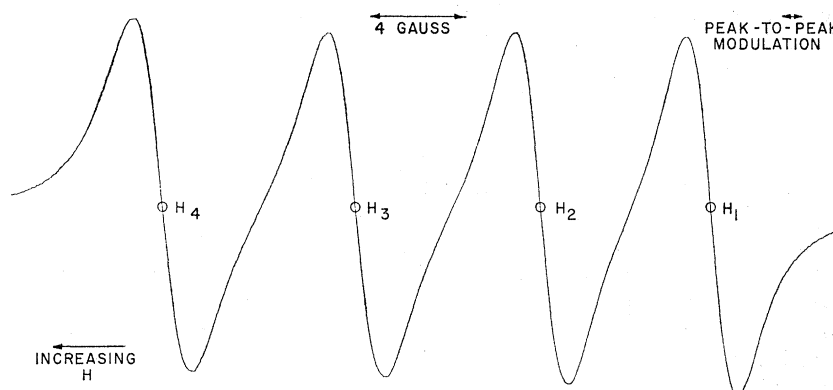
The resonance lamp was a Cario-Lockte-Holtgreven-type flow lamp of a design developed by Lurio and Novick.<sup>11</sup> Lithium evaporated from a small stainless steel oven is prevented from coating the exit window of the quartz envelope by a continuous flow of argon. The argon also serves to carry the discharge produced by an rf voltage applied between the oven and a conducting ring outside the quartz envelope. An Eico 720 transmitter operating at a frequency of 7 Mc/sec was used for the rf source. Typical spectral characteristics of the light emitted by such a lamp for various oven temperatures and gas pressures are discussed in Ref. 11.

The choice of an atomic beam as the scatterer was dictated by the fact that lithium reacts rapidly with Pyrex, quartz, and even sapphire at the temperatures required to maintain the necessary vapor pressure of lithium in an isothermal enclosure.<sup>12</sup> With an oven temperature of  $420^\circ\text{C}$  the lithium density in the scattering volume was approximately  $10^{11}$  atoms/cc. This was sufficient to give large crossing signals and yet low enough that coating of the windows by atoms scattered out of the beam was negligible. The combined effects of a small diffusion pump, a long pumping line, and no special care taken to avoid contamination of the vacuum system resulted in a vacuum which was probably not much better than  $10^{-3}$  Torr in the scattering chamber. That this poor vacuum caused no problems is testimony to the ease of performing level-crossing measurements as contrasted with optical double reso-

<sup>11</sup> B. Budick, R. Novick, and A. Lurio, Appl. Opt. 4, 229 (1965).

<sup>12</sup> Recently, however, encouraging results have been obtained at Columbia [Columbia Radiation Laboratory Progress Report, 1964 (unpublished)] and in our laboratory (private communication from V. J. Slabinski) from lithium resonance cells constructed with heated windows of MgO and CaF<sub>2</sub>.

FIG. 4. Recorder trace of the derivative of the low-field crossing signal in the  $2^2P$  term of  $\text{Li}^7$ .



nance measurements, where a high vacuum is necessary to avoid rf discharges. The accumulated data taking time between reloadings of the oven was typically 12 to 16 h.

Extensive mapping of the magnetic field in the median plane of the atomic beam with the proton probe revealed a roughly elliptical area of approximately  $1\frac{1}{8}$  in. by  $\frac{3}{4}$  in. within which the magnetic field was homogeneous to a part in  $10^5$ , provided the field strength was first raised a few thousand gauss above that of the crossing and then lowered to it. The inhomogeneity perpendicular to this plane was well within a part in  $10^5$  over the height of the beam. With the volume of intersection of the atomic beam and incident light beam centered in this area of maximum homogeneity, at least 95% of the light scattering took place in a region where the magnetic field was uniform to one part in  $10^5$ . Field-warping effects of the atomic-beam apparatus itself were shown to be within a part in  $10^5$  by observing the proton resonance signal in water doped with  $\text{MnCl}_2$  as the apparatus was moved into the magnet gap and the oven-heating current turned on.

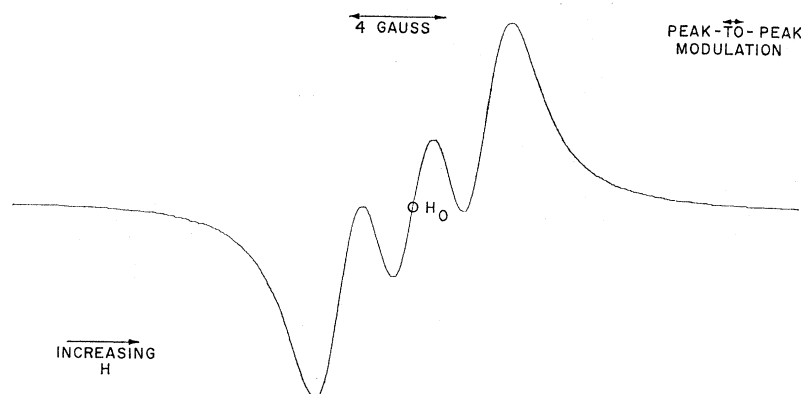
The RCA 7326 photomultiplier in combination with a Corning 2-59 glass filter had a spectral response which peaked at approximately 6400 Å and dropped to essentially zero at 6200 and 7400 Å. Relative transmission

at the 6708 Å line ( $2P$  to  $2S$  transition) of lithium was about 80%. The total photomultiplier signal was monitored by displaying the voltage across the 1-MΩ anode load resistor of the photomultiplier circuit on one beam of a dual-beam oscilloscope. The magnetic field was modulated at 40 cycles/sec and the ac component of the photomultiplier signal was capacitatively coupled to the input of a 40 cycles/sec lock-in detector. The output of the tuned amplifier of the lock-in was monitored on the second beam of the oscilloscope and the demodulated signal was recorded with a strip chart recorder. Both the total signal on the chart recorder and the amplitude of the 40 cycle/sec signal on the oscilloscope were proportional, for low amplitude modulation of the magnetic field, to the magnetic field derivative of the detected light signal. Typical recorder traces of the derivative of the low-field crossing signal in the  $2^2P$  term of  $\text{Li}^7$  and  $\text{Li}^6$  are shown in Figs. 4 and 5.

The proton probe was powered by a transistorized marginal oscillator<sup>13</sup> whose frequency was measured on a Hewlett-Packard 524B frequency counter. Frequent comparisons between the crystal oscillator of the counter and WWV demonstrated a long-term stability for this counter of a few parts in  $10^6$ .

For the geometry of Fig. 3, where the directions of both the incident and detected light beams are per-

FIG. 5. Recorder trace of the derivative of the low-field crossing signal in the  $2^2P$  term of  $\text{Li}^6$ .



<sup>13</sup> B. Donnally and T. M. Sanders, Jr., Rev. Sci. Instr. 31, 977 (1960).

pendicular to the magnetic field  $\mathbf{H}$ , the low-field crossing signal is proportional to  $\sin^2\theta_1 \sin^2\theta_2$ , where  $\theta_1$  and  $\theta_2$  are the angles between  $\mathbf{H}$  and the planes of polarization of the incident and detected light. Thus, the signal is a maximum for the incident and detected light both polarized perpendicular to  $\mathbf{H}$  ( $\theta_1 = \theta_2 = \pi/2$ ). Since an unpolarized light beam is equivalent to an incoherent superposition of two beams of equal intensity, one polarized parallel and one perpendicular to  $\mathbf{H}$ , a crossing signal could be observed with unpolarized light. However, the polarization parallel to  $\mathbf{H}$  contributes nothing to the crossing signal, while adding to the background signal and, therefore, to the noise. All of the data reported here were obtained with  $\theta_1 = \theta_2 = \pi/2$ .

The isotopic abundances of natural lithium are approximately 93%  $\text{Li}^7$  and 7%  $\text{Li}^6$ . Separated isotopes were used in both the resonance lamp and the atomic beam for the measurements on  $\text{Li}^7$  as well as those on  $\text{Li}^6$  to avoid even small distortions of the crossing signal by the signal from the other isotope. For  $\text{Li}^6$  the isotope separation was 99% and for  $\text{Li}^7$  99.99%.

#### IV. DATA TAKING PROCEDURE

Figures 4 and 5 show that the low-field crossing signals are superpositions of Lorentzian signals from each of the observable hyperfine crossings, four for  $\text{Li}^7$  ( $I = \frac{3}{2}$ ) and three for  $\text{Li}^6$  ( $I = 1$ ). The component signals are quite well resolved in  $\text{Li}^7$ , but poorly resolved in  $\text{Li}^6$ . This poorer resolution in  $\text{Li}^6$  is to be expected, since the magnetic hyperfine interaction constants of  $\text{Li}^6$  are a factor of  $g_I(\text{Li}^6)/g_I(\text{Li}^7) \approx \frac{2}{3}$  smaller than those of  $\text{Li}^7$ . All of the data were taken with low modulation amplitudes, short time constants, and slow sweep rates, thus avoiding any appreciable distortion of the signals from these familiar instrumental sources. In devising procedures for taking and analyzing precise data, we have considered three instrumental effects which we feel are the most important possible sources of distortion of the signals. The first two of these are associated with the fact that the radiation from the resonance lamp covers only a rather small spectral range. As the magnetic field strength is varied the Zeeman levels of the beam atoms are tuned over the spectral distribution of the lamp. Therefore, there can be changes in the detected signal arising from a slow variation of the background signal from the levels that are not crossing, and from a slow variation of the lamp intensity over the spectral width of the crossing [i.e., variation of the "constant"  $c$  in Eq. (7)]. A third source of instrumental error is the admixture of a small dispersion-type lineshape into the predominantly Lorentzian line shape because of a small departure of the average scattering angle from  $90^\circ$ . That the first of these three effects (sloping background) produced at most a linear variation over the region of the crossing is apparent from Figs. 4 and 5, since the baseline of these derivative signals is the same above the crossing region as below. Actually, the sloping

background effect was shown to be negligible in both  $\text{Li}^6$  and  $\text{Li}^7$  by observing that the 40 cycles/sec signal from the narrow-band amplifier dropped to zero both above and below the crossing. In Appendix C1 it is shown that the type of distortion of the crossing signal produced by the second effect is the same to first order as that produced by the third.

For  $\text{Li}^7$ , it was not necessary to apply corrections for signal distortion to the measured positions of all four of the crossings, since the *intervals* between the crossings proved to be extremely insensitive to experimental conditions (atomic beam density, alignment of the lamp, magnetic field homogeneity, etc.). In fact, we were able to determine the intervals between hyperfine crossings with an uncertainty approximately ten times smaller than that ultimately assigned to the field strengths of the crossings. Hence, precise measurements of the crossing fields were limited to the central pair of crossings (labeled  $H_2$  and  $H_3$  in Fig. 4). The positions of  $H_2$  and  $H_3$  were located by finding the corresponding minima in the modulation signal and then using the observed magnitudes of the four central derivative peaks displayed on the chart recorder to calculate corrections to the measured positions. The details of this calculation are given in Appendix C1. A measurement of the intervals consisted of locating in succession the fields  $H_1$  through  $H_4$  (or  $H_4$  through  $H_1$ ) by manually adjusting the field strength until a sharp minimum in the modulation signal was observed on the oscilloscope and then measuring the field with the proton probe.

For  $\text{Li}^6$ , measurements were restricted to a precise determination of the position of the central peak (central zero of the derivative signal, labeled  $H_0$  in Fig. 5). No attempt was made to analyze the hyperfine structure of the  $\text{Li}^6$  signal, since no information would be obtained which could not be calculated from the  $\text{Li}^7$  data and the known ratios of the magnetic dipole and electric quadrupole moments. The position of  $H_0$  was found from the minimum of the modulation signal and from pairs of recorder traces (one sweeping up in field and the other down) calibrated with proton frequency markers. The measured positions were corrected using the observed magnitudes of the two large derivative peaks in Fig. 5.

#### V. EXPERIMENTAL RESULTS AND ANALYSIS

##### A. Fine-Structure Splittings

The data used to determine  $H_2$  and  $H_3$ , the magnetic field strengths corresponding to the second and third hyperfine components of the low-field crossing in  $\text{Li}^7$ , are given in Table I.  $\Delta H_2$  and  $\Delta H_3$  are corrections calculated from the differences in the magnitudes of the positive and negative derivative peaks of the given hyperfine crossing signal as discussed in Appendix C1. Column six of Table I shows that  $\Delta H_2$  is consistently less than  $\Delta H_3$  by approximately 0.15 kc/sec. This dif-

TABLE I. Measured values of  $H_2$  and  $H_3$  and corrections for difference in magnitudes of derivative peaks, all in kc/sec on the proton probe.

Run No.	$H_2$	$H_3$	$\Delta H_1$	$\Delta H_2$	$\Delta H_3 - \Delta H_2$	$(\Delta H_2 + \Delta H_3)/2$	$H_2$ (corr.)	$H_3$ (corr.)
1	13 573.80	13 606.11	+0.10	+0.31	+0.21	+0.20	13 574.00	13 606.31
2	4.24	6.56	-0.54	-0.40	+0.14	-0.47	3.77	6.09
3	4.28	6.64	-0.40	-0.24	+0.16	-0.32	3.96	6.32
	4.08	6.42	-0.41	-0.32	+0.09	-0.36	3.72	6.06
	3.88	6.18	-0.58	-0.40	+0.18	-0.49	3.39	5.69
4	3.67	6.03	-0.10	0	+0.10	-0.05	3.62	5.98
	3.64	5.98	-0.18	0	+0.18	-0.09	3.55	5.89
5	3.66	6.02	-0.10	+0.05	+0.15	-0.02	3.64	6.00

ference is caused by the slight overlap of the signals from the four hyperfine crossings. Even if there is no distortion of the crossing signal from the instrumental effects considered in Appendix C1, the overlap will distort the signal from the second hyperfine crossing by increasing the magnitude of the lower field derivative peak and decreasing that of the higher field derivative peak, and will produce just the opposite distortion of the signal for the third hyperfine crossing. A value of 0.15 kc/sec for  $\Delta H_3 - \Delta H_2$  corresponds to a difference in the sizes of the derivative peaks of slightly more than 2% and agrees with our estimates of the effect of overlap on the sizes of these peaks. The effect of overlap on the positions of  $H_1$  through  $H_4$  can be calculated directly, as we shall show presently. For now we are concerned only that we do not introduce false corrections to  $H_2$  and  $H_3$  by interpreting all of the distortion of the derivative peaks as being due to the instrumental effects of Appendix C1. Thus, the appropriate corrections to be added to the measured  $H_2$  and  $H_3$  is the average of  $\Delta H_2$  and  $\Delta H_3$  given in column seven of Table I.

Averaging the corrected values of  $H_2$  and  $H_3$ , we obtain

$$H_2 = 13573.71 \pm 0.20 \text{ kc/sec,}$$

$$H_3 = 13606.04 \pm 0.21 \text{ kc/sec,}$$

where the uncertainties are standard deviations. These uncertainties are consistent with our estimates for the precision with which we could determine the measured field values and the corrections for instrumental effects. The entries in columns two and three of Table I are in most instances averages of the results for several settings of the null of the modulation signal with spreads of typically 0.10 kc/sec. The uncertainty in the position of the baseline from which derivative peak heights were measured was about one chart division and corresponded to an uncertainty of 0.20 kc/sec in the value of  $\Delta H$ . It should be noted that the uncertainty in baseline position does not affect the value of  $\Delta H_3 - \Delta H_2$ . This explains the small standard deviation of only 0.04 kc/sec for this quantity and the fact that  $H_3 - H_2$

equals 32.33 kc/sec in very good agreement with the more precise measurement of this interval given below.

Table II gives the data used to determine  $H_0$ , the center of the low-field crossing in  $\text{Li}^6$ . The value of  $\Delta H_0$  was determined from the difference in the magnitudes of the large derivative peaks of Fig. 5 as explained in Appendix C1. Averaging the corrected values of  $H_0$ , we obtain

$$H_0 = 13589.66 \pm 0.22 \text{ kc/sec.}$$

For the  $\text{Li}^6$  signal, an uncertainty in the position of the baseline of one chart division corresponds to an uncertainty in  $\Delta H_0$  of about 0.35 kc/sec.

Before the above field strengths can be simply related to the fine structure splittings in  $\text{Li}^6$  and  $\text{Li}^7$  using the theory developed in Sec. II, they must be corrected for shifts of the hyperfine levels by the off-diagonal matrix elements of the magnetic hyperfine interaction. These shifts are small and can be treated by second-order perturbation theory using the off-diagonal matrix elements given in Appendix A. The values of  $\alpha(1/r^3)$  and  $\xi$  needed to evaluate these matrix elements were obtained, as discussed below, from Ritter's number for the zero-field hyperfine splitting in the  $2^2P_{1/2}$  state and the average of the measured intervals  $H_2 - H_1$ ,  $H_3 - H_2$ , and  $H_4 - H_3$ . Having found the corrections to  $H_1$

TABLE II. Measured values of  $H_0$  and corrections for difference in magnitudes of derivative peaks, all in kc/sec on the proton probe.

Run No.	$H_0$	$\Delta H_0$	$H_0$ (corr.)
6	13 590.20 <sup>a</sup>	-0.52	13 589.68
	90.16 <sup>b</sup>	-0.55	9.61
	90.18 <sup>b</sup>	-0.53	9.65
7	89.28 <sup>b</sup>	+0.69	9.97
	89.27 <sup>b</sup>	+0.52	9.79
	89.39 <sup>a</sup>	+0.45	9.84
8	89.67 <sup>a</sup>	-0.23	9.44
	89.67 <sup>a</sup>	-0.38	9.29

<sup>a</sup> Determined by manual settings on central zero of derivative signal.  
<sup>b</sup> Determined from a pair of recorder traces.

TABLE III. Further corrections to the measured fields, all in kc/sec on the proton probe.

	Correction for off-diagonal dipole matrix elements	Correction for overlap	Total correction
$H_1$	-0.36	-0.134	-0.494
$H_2$	+0.24	-0.015	+0.225
$H_3$	+0.58	+0.015	+0.595
$H_4$	+0.63	+0.134	+0.764
$H_0$	+0.033	0	+0.033

through  $H_4$ , one should repeat the correction calculation using the corrected intervals. However, the initial corrections were small enough to make this repeat of the calculation unnecessary. The corrections to the  $H_i$  arising from the off-diagonal matrix elements of the dipole interaction are tabulated in the second column of Table III. Finally, overlap of the signals from the four hyperfine components of the low-field crossing in  $\text{Li}^7$  causes small shifts in the positions of the  $H_i$ . The calculation of these shifts is discussed in Appendix C2 and their values given in column three of Table III. In addition to all of the corrections considered above, we have investigated three additional perturbations of the level positions and found their effects to be negligible compared to the uncertainty of the data. These were: (1) off-diagonal matrix elements of the quadrupole interaction; (2) a change in the excitation matrix elements over the region of the crossing, i.e., a variation of  $B$  in Eq. (7); (3) curvature of the Zeeman levels in the region of the crossing. Applying the corrections in column four of Table III to the above values of  $H_2$ ,  $H_3$ , and  $H_0$ , we obtain for the final corrected positions of these crossing fields

$$H_2' = 13573.94 \pm 0.30 \text{ kc/sec,}$$

$$H_3' = 13606.64 \pm 0.30 \text{ kc/sec,}$$

$$H_0' = 13589.69 \pm 0.30 \text{ kc/sec,}$$

where the uncertainties represent 80% confidence limits.

The fine-structure splitting  $\delta W_0$  is related to  $H_L$  by Eq. (2a), where  $H_L$  is the field at which the low-field crossing would occur in the absence of any hyperfine interaction. For  $\text{Li}^7$ ,  $H_L$  is equal to  $H_2'$ , plus one-half the interval  $H_3' - H_2'$ , minus 0.035 kc/sec to correct for a small shift of  $H_2'$  by the quadrupole interaction. For  $\text{Li}^6$ ,  $H_L$  is equal to  $H_0'$ , the correction for the quadrupole interaction being entirely negligible. Thus,

$$H_L(\text{Li}^7) = 13590.2 \pm 0.3 \text{ kc/sec,}$$

$$H_L(\text{Li}^6) = 13589.7 \pm 0.3 \text{ kc/sec.}$$

The corresponding values of  $\delta W_0$  are

$$\delta W_0(\text{Li}^7) = 10053.24 \pm 0.22 \text{ Mc/sec,}$$

$$\delta W_0(\text{Li}^6) = 10052.76 \pm 0.22 \text{ Mc/sec.}$$

In calculating  $\delta W_0$  from  $H_L$ , we have taken  $\mu_0 H_L$  to be  $328.7319 \pm 0.0006$  times the value of  $H_L$  expressed as a frequency reading of our proton probe,<sup>14</sup>  $g_S = 2.00232$ , and  $g_L = 1 - m/M$ , where  $m$  is the electron mass and  $M$  the nuclear mass. The stated uncertainty in  $\delta W_0$  is solely that arising from the experimental uncertainty in  $H_L$ . No attempt has been made to modify the above expression for  $g_L$  for relativistic and diamagnetic corrections.<sup>15</sup> Such corrections could change the values of the fine-structure splittings by several parts in  $10^5$ . However, we are not convinced that the effort involved in making such a difficult set of calculations is warranted at this time. Even if the corrections can be made, the uncertainty in our measurement offers little hope of improving on the present value of the fine structure constant  $\alpha$ .

### B. Magnetic Hyperfine Constants of the $2^2P$ term of $\text{Li}^7$

The three magnetic field intervals between the four hyperfine components of the low-field  $\text{Li}^7$  crossing signal were determined from a total of 135 separate measurements of each of the crossing fields  $H_1$ ,  $H_2$ ,  $H_3$ , and  $H_4$ . These measurements were made on 8 days spread over a time interval of 3 weeks, with various lamp and beam conditions. There was no evidence of any dependence on lamp and beam parameters, the variations in measured intervals from one day to the next lying within the scatter of a given days data. The averages of these measurements, expressed as frequency intervals on the proton probe, are

$$H_2 - H_1 = 31.99 \pm 0.033 \text{ kc/sec,}$$

$$H_3 - H_2 = 32.31 \pm 0.030 \text{ kc/sec,}$$

$$H_4 - H_3 = 32.40 \pm 0.054 \text{ kc/sec,}$$

where the uncertainties are standard deviations. We have no explanation for the appreciably larger uncertainty of the last interval. These *measured* intervals were the ones used to calculate the off-diagonal magnetic dipole corrections to the values of the  $H_i$  that are discussed above and tabulated in column two of Table III. The *corrected* intervals (corrected for the effects of the off-diagonal dipole interaction and for overlap of the four hyperfine signals) are obtained by applying the corrections given in column four of Table III to the measured intervals. They are

$$H_2' - H_1' = 32.71 \pm 0.04 \text{ kc/sec,}$$

$$H_3' - H_2' = 32.68 \pm 0.04 \text{ kc/sec,}$$

$$H_4' - H_3' = 32.57 \pm 0.06 \text{ kc/sec,}$$

where the uncertainties represent 80% confidence limits.

<sup>14</sup> R. D. Kaul, Ph.D. thesis, Case Institute of Technology, 1963 (unpublished).

<sup>15</sup> A. Abragam and J. H. VanVleck, Phys. Rev. **92**, 1448 (1953).

The constants  $\alpha\langle 1/r^3 \rangle$  and  $\xi$  can be determined from the average of the corrected magnetic field intervals and Ritter's value for the zero-field hyperfine splitting in the  $2^2P_{1/2}$  state of  $\text{Li}^7$ . If we consider only the diagonal matrix elements of  $\mathcal{H}_D$ , the three magnetic field intervals should be equal, with a value that can be calculated from the difference between the diagonal matrix elements of  $\mathcal{H}_D$  in the  $|\frac{1}{2}, \frac{1}{2}, m_I\rangle$  and  $|\frac{3}{2}, -\frac{3}{2}, m_I\rangle$  states and the difference in the slopes of these levels at the crossing. The third term on the right-hand side of Eq. (3) shifts both levels of the same  $m_I$  by equal amounts and, therefore, does not change the field strength at which a given hyperfine crossing occurs. As we shall see below, the diagonal quadrupole interaction does alter the values of  $H_2' - H_1'$  and  $H_4' - H_3'$ , but by amounts that are equal in magnitude and opposite in sign for these two intervals. Therefore, there is no change in the average of the three intervals. The shifts in the  $H_i$  from the off-diagonal matrix elements of  $\mathcal{H}_D$  have already been corrected for, and the effects of the off-diagonal matrix elements of  $\mathcal{H}_Q$  are negligible. Taking the relevant matrix elements from Appendix A, we obtain

$$(24/11)\alpha\langle 1/r^3 \rangle + (2/11)\xi = 23.42 \pm 0.02 \text{ Mc/sec},$$

where the average of the three magnetic field intervals has been converted to a frequency interval using 3.054 Mc/G for  $\partial\Delta/\partial H$ , the rate at which the levels cross, and 4.2577 kc/G for the conversion factor between proton resonance frequency and magnetic field strength.

At  $H=0$ , the matrix element  $\langle \frac{1}{2}, \frac{1}{2}, m_I | \mathcal{H}_D | \frac{1}{2}, \frac{1}{2}, m_I \rangle$  is equal to  $\frac{1}{2}m_I[(8/3)\alpha\langle 1/r^3 \rangle - \frac{1}{3}\xi]$ . This is just the  $m_J = +\frac{1}{2}$  diagonal matrix element of the hyperfine interaction in the  $2^2P_{1/2}$  state when this interaction is expressed in the  $m_J, m_I$  representation. The quantity in brackets is the familiar hyperfine constant  $a_{1/2}$ , whose value for the  $2^2P$  term of  $\text{Li}^7$  has been determined by Ritter.<sup>5</sup> Thus,

$$(8/3)\alpha\langle 1/r^3 \rangle - \xi/3 = 46.17 \pm 0.35 \text{ Mc/sec}.$$

From these two equations we deduce

$$\begin{aligned} \alpha\langle 1/r^3 \rangle &= 13.37 \pm 0.05 \text{ Mc/sec} \\ \xi &= -31.6 \pm 0.7 \text{ Mc/sec}. \end{aligned}$$

### C. Quadrupole Moment of $\text{Li}^7$

A value for the quadrupole moment of  $\text{Li}^7$  can be obtained from the differences in the three magnetic field intervals. The matrix elements of Appendix B predict shifts in the positions of the hyperfine crossings that change  $H_2' - H_1'$ ,  $H_3' - H_2'$ , and  $H_4' - H_3'$  by the amounts  $-(3/11)b/(\partial\Delta/\partial H)$ , 0, and  $+(3/11)b/(\partial\Delta/\partial H)$ , respectively, where  $b = \frac{2}{3}e^2Q\langle 1/r^3 \rangle$ . The observed differences between the first and second and the second and third field intervals yield

$$b = -0.18 \pm 0.12 \text{ Mc/sec}.$$

When this value for  $b$  is combined with the  $\langle 1/r^3 \rangle$

obtained from the above result for  $\alpha\langle 1/r^3 \rangle$ , we have

$$Q(\text{Li}^7) = (-3 \pm 2) \times 10^{-26} \text{ cm}^2.$$

No correction has been made for core-shielding effects of the type considered by Sternheimer,<sup>16</sup> since it is not obvious that the  $\langle 1/r^3 \rangle$  obtained from our UHF analysis does not already include a contribution from the polarized core. In any event, any core-shielding correction to the above value for  $Q(\text{Li}^7)$  will be a small fraction of our experimental uncertainty.

### D. Lifetime of the $2^2P$ Term of Li

The lifetime  $\tau$  of the  $2^2P$  term of Li can be determined from the peak-to-peak derivative width of the signal obtained from a single hyperfine component of the low-field crossing in  $\text{Li}^7$ . However, the experimental arrangements used in this investigation are less than ideal for a determination of  $\tau$ , since the nonuniformity of particle density in the spreading atomic beam makes it difficult to estimate the amount of coherence narrowing<sup>17</sup> of the crossing signal. Therefore, it did not seem worthwhile to devote an appreciable amount of time to this measurement. A single recorder tracing of the low-field crossing signal in  $\text{Li}^7$  was taken with a number of frequency markers in the vicinity of each of the eight derivative peaks. Values of 9.68, 9.63, 9.55, 9.41 kc/sec were obtained for the peak-to-peak derivative widths of the signals from the four hyperfine crossings, each with an uncertainty of 3% determined by the difficulty of estimating the positions of the maxima and minima of the recorder trace.

From Eq. (7) and the definition of  $\gamma$  in terms of  $\tau$ , it follows that the peak-to-peak derivative width of a Lorentz crossing signal is equal to  $[\sqrt{3}\pi\tau(\partial\Delta/\partial H)]^{-1}$ , where  $\partial\Delta/\partial H$  is the rate at which the levels cross. The average of the above values for the peak-to-peak derivative widths of the four hyperfine components of the low-field crossing signal in  $\text{Li}^7$  is  $9.57 \pm 0.14$  kc/sec. When corrected for modulation broadening,<sup>18</sup> this average width yields a lifetime of  $(2.78 \pm 0.04) \times 10^{-8}$  sec. The linewidth data were taken with a sufficiently short time constant in the detector circuit and slow sweep rate of the magnetic field to avoid significant broadening from this source. However, overlap of the four hyperfine signals *reduces* the derivative width of each of the two outer signals by 1.4% and of each of the two inner signals by 2.7%. Thus, the effect of overlap is to reduce the average derivative width by 2%, and the above value for  $\tau$  must be corrected by decreasing it by the same percentage giving

$$\tau = (2.72 \pm 0.04) \times 10^{-8} \text{ sec}.$$

This result is in excellent agreement with Heavens's<sup>19</sup> theoretical value of  $2.72 \times 10^{-8}$  sec, indicating that

<sup>16</sup> R. M. Sternheimer, Phys. Rev. **84**, 244 (1951).

<sup>17</sup> J. P. Barrat, J. Phys. Radium **20**, 541 (1959); **20**, 633 (1959); **20**, 657 (1959).

<sup>18</sup> H. Wahlquist, J. Chem. Phys. **35**, 1708 (1961).

<sup>19</sup> O. S. Heavens, J. Opt. Soc. Am. **51**, 1058 (1961).

there was no appreciable coherence narrowing of the crossing signal.

## VI. DISCUSSION

### A. Fine-Structure Splitting

Previous measurements of the fine structure of the  $2^2P$  term of Li have all used the techniques of conventional optical spectroscopy. The results of the most precise of these optical measurements are compared with the present results in Table IV. Only Hughes's<sup>20</sup> experiment was performed using separated isotopes, which avoids the difficulty of interpreting a pattern of overlapping spectral lines resulting from the presence of both isotopes.

The normal mass effect, which contracts the energy-level spectrum of the atom by the ratio of the reduced mass to the electronic mass, predicts that  $\delta W_0(\text{Li}^6)$  should be less than  $\delta W_0(\text{Li}^7)$  by slightly more than one part in  $10^5$ . Our value of  $\delta W_0$  for  $\text{Li}^6$  is less than that for  $\text{Li}^7$  by almost five parts in  $10^5$ , but this difference is only slightly greater than the sum of the experimental uncertainties in these two numbers. Also, the values of  $g_L$  used in Eq. (2a) to calculate  $\delta W_0$  from  $H_L$  have not been corrected for relativistic and diamagnetic effects. Thus, no meaningful estimate can be made of the specific mass<sup>20</sup> contribution to the fine-structure splitting.

### B. Magnetic Hyperfine Constants

Goodings's<sup>3</sup> calculated values for the magnetic dipole interaction constants in the  $2^2P$  term of  $\text{Li}^7$  are

$$a_{d3/2} = 6.5 \text{ Mc/sec,}$$

$$a_{c3/2} = -10.7 \text{ Mc/sec.}$$

Equation (6) and the measured values of  $\alpha\langle 1/r^3 \rangle$  and  $\xi$  yield

$$a_{d3/2} = 7.13 \pm 0.03 \text{ Mc/sec,}$$

$$a_{c3/2} = -10.53 \pm 0.23 \text{ Mc/sec.}$$

The discrepancy between the experimental and theoretical values for  $a_{d3/2}$  is very likely the result of Goodings's neglect of the effect of correlation on the wave function of the  $p$  electron. The agreement of the experimental and theoretical values for  $a_{c3/2}$  is strong support

TABLE IV. Fine-structure splittings in the  $2^2P$  term of  $\text{Li}^7$  and  $\text{Li}^6$  in Mc/sec.

	$\text{Li}^7$	$\text{Li}^6$
Jackson and Kuhn <sup>a</sup>	10 109 $\pm 15$	9503
Meissner <i>et al.</i> <sup>b</sup>	10 073 $\pm 15$	
Hughes <sup>c</sup>	10 103 $\pm 90$	10 103 $\pm 90$
Brog <i>et al.</i>	10 053.24 $\pm 0.22$	10 052.76 $\pm 0.22$

<sup>a</sup> D. A. Jackson and H. Kuhn, Proc. Roy. Soc. (London) **A173**, 278 (1939).

<sup>b</sup> K. W. Meissner, L. G. Mundie, and P. H. Stelson, Phys. Rev. **74**, 932 (1948).

<sup>c</sup> See Ref. 20.

<sup>20</sup> R. H. Hughes, Phys. Rev. **99**, 1837 (1955).

for the adequacy of UHF calculations of Fermi contact contributions to the hyperfine interaction in the  $P$  states of atomic lithium.

A more striking confirmation of the validity of our analysis is provided in the following paper, where it is shown that the matrix element responsible for the anticrossing of neighboring hyperfine levels in the high-field crossing regions of  $\text{Li}^7$  and  $\text{Li}^6$  can be obtained from the width of the anticrossing signal and also calculated directly from the magnetic hyperfine interaction constants. To state that the agreement between these two values for the anticrossing matrix element is well within the experimental uncertainties does not do justice to the calculation. It is more pertinent to explain that if the magnitude of  $\xi$  is decreased by 5% and that of  $\alpha\langle 1/r^3 \rangle$  is increased to restore agreement between the calculated and experimental values of  $a_{1/2}$ , the two values for the anticrossing matrix element differ by more than the sum of their uncertainties. This result we present as our strongest evidence that the analysis of the hyperfine structure data is essentially correct, and that the measured value of  $\xi$  does indeed represent the Fermi contact contribution to the hyperfine interaction. We will not attempt to answer the question of whether the Fermi contact term is the result of a real core-splitting induced by exchange or is to be explained as an effect of angular correlation.

Budick *et al.*,<sup>21</sup> have investigated the  $3^2P$  term and Isler, Marcus, and Novick<sup>22</sup> the  $4^2P$  term of  $\text{Li}^7$ . Both these investigations employed the level-crossing technique. The average spacings of the hyperfine components of the low-field crossing signals in the  $2P$ ,  $3P$ , and  $4P$  terms are in the ratios 1:0.2946:0.1239. The corresponding proportions for  $(1/n^*)^3$  are 1:0.2942:0.1233, where  $n^*$  is the effective quantum number of the term. One would expect the constant  $\alpha\langle 1/r^3 \rangle$  to scale very nearly as  $(1/n^*)^3$ . The fact that the average spacings scale in the same manner shows that  $\xi$ , the core polarization contribution to the hyperfine interaction, is also proportional to  $(1/n^*)^3$  for the  $P$  terms of Li.

In view of the uncertainties involved in using Eq. (2a) to calculate  $\delta W_0$  from  $H_L$ , it would appear worthwhile to consider a more direct measurement of  $\delta W_0$  by a low-field optical-double-resonance (ODR) experiment. However, even putting aside the problems inherent in an ODR experiment at 10 Gc/sec in a state with a  $\tau$  as short as  $2.7 \times 10^{-8}$  sec, the prospect for obtaining a precise value for  $\delta W_0$  by an ODR investigation is not good. The dipole interaction constant in the  $2^2P_{3/2}$  state of  $\text{Li}^7$  is equal to

$$a_{d3/2} + a_{c3/2} = -3.40 \pm 0.23 \text{ Mc/sec.}$$

<sup>21</sup> B. Budick, H. Bucka, R. Goshen, A. Landman, and R. Novick, Phys. Rev. **147**, 1 (1966). A. Landman, Ph.D. thesis, Columbia University, 1963 (unpublished).

<sup>22</sup> R. C. Isler, S. Marcus, and R. Novick, Bull. Am. Phys. Soc. **10**, 1096 (1965).

This is to be compared with a value of at least 11.7 Mc/sec for the full width at half-maximum of the ODR signal associated with a transition between any two levels of the  $2^2P$  term of  $\text{Li}^7$ . Thus, there would be a large overlap of the ODR signals from neighboring levels of the  $2^2P_{3/2}$  state, and it is unlikely that one could determine the fine-structure splitting to much better than one Mc/sec.

### C. Quadrupole Moment

Our value for  $Q(\text{Li}^7)$  agrees, within the large error limits, with the value of  $-4.5 \times 10^{-26}$  cm<sup>2</sup> calculated by Kahalas and Nesbet from the quadrupole coupling constant in  $\text{Li}^7\text{H}$  measured by Wharton, Gold, and Klemperer.<sup>8</sup> A recent determination of  $Q(\text{Li}^7)$  by Isler, Marcus, and Novick<sup>23</sup> from level-crossing measurements in the  $3^2P$  term is now known to be in error.<sup>24</sup> The uncertainty in the molecular value for  $Q$  arises almost entirely from the uncertainty in the calculated value of the electric field gradient at the lithium nucleus in  $\text{LiH}$ . This uncertainty is difficult to estimate reliably, but is probably less than 10%. The atomic value for  $Q$  is derived from the ratio of the quadrupole coupling constant  $b$  to the dipole constant  $\alpha\langle 1/r^3 \rangle$ , which avoids the necessity of having a detailed knowledge of the atomic wave function. Since the atomic value for  $Q$  is free of the computational uncertainties of the molecular value, it would be desirable to improve the experimental precision of the atomic measurements. However, the difficulty of making any substantial inroads in this direction can be appreciated when one notes that the changes due to the quadrupole interaction in the spacings of the hyperfine components of the low-field crossing in  $\text{Li}^7$  are only about 1% of the peak-to-peak derivative width of an individual hyperfine crossing signal.

### ACKNOWLEDGMENTS

We wish to thank R. D. Kaul for aid in the initial stages of this experiment, R. Novick and A. Lurio for supplying us with a design for the resonance lamp used in this work, and P. A. Franken for several informative discussions on the nature of level-crossing signals. We are especially indebted to L. L. Foldy for help in formulating an adequate treatment of the hyperfine-structure data.

### APPENDIX A: MAGNETIC DIPOLE MATRIX ELEMENTS

To reduce the hyperfine-structure data, we require the matrix elements of the magnetic dipole operator  $\mathcal{H}_D$  for a one-electron  $P$  state. With  $\mathcal{H}_D$  given by Eq. (5), these matrix elements are most easily evaluated using wave functions in the  $m_L, m_S, m_I$  representation. The actual wavefunctions are eigenfunctions of  $F_z$

$= J_z + I_z$  and, since we are in the extreme *hyperfine* Paschen-Back region, they are very nearly eigenfunctions of  $J_z$  and  $I_z$ , separately. We shall adopt the  $J, m_J, m_I$  representation ( $J$ , which is not a good quantum number, refers to the  $H=0$  state from which the given state is derived by slowly increasing the magnetic-field strength) and treat the small off-diagonal terms using second-order perturbation theory. This perturbation treatment is adequate except for field strengths corresponding to the close approach of two levels with the same  $m_F$ , such as occurs at the high-field crossing. Then, as discussed in the following paper, it is necessary to diagonalize the two by two submatrix of these  $m_F$  levels.

For a one-electron  $P$  state the transformations between the  $J, m_J, m_I$  and  $m_L, m_S, m_I$  representations are

$$\begin{aligned} \left| \frac{3}{2}, \frac{3}{2}, m_I \right\rangle &= \left| 1, \frac{1}{2}, m_I \right\rangle, \\ \left| \frac{3}{2}, \frac{1}{2}, m_I \right\rangle &= A \left| 0, \frac{1}{2}, m_I \right\rangle + B \left| 1, -\frac{1}{2}, m_I \right\rangle, \\ \left| \frac{3}{2}, -\frac{1}{2}, m_I \right\rangle &= C \left| -1, \frac{1}{2}, m_I \right\rangle + D \left| 0, -\frac{1}{2}, m_I \right\rangle, \\ \left| \frac{3}{2}, -\frac{3}{2}, m_I \right\rangle &= \left| -1, -\frac{1}{2}, m_I \right\rangle, \\ \left| \frac{1}{2}, \frac{1}{2}, m_I \right\rangle &= -B \left| 0, \frac{1}{2}, m_I \right\rangle + A \left| 1, -\frac{1}{2}, m_I \right\rangle, \\ \left| \frac{1}{2}, -\frac{1}{2}, m_I \right\rangle &= -D \left| -1, \frac{1}{2}, m_I \right\rangle + C \left| 0, -\frac{1}{2}, m_I \right\rangle. \end{aligned}$$

$A, B, C,$  and  $D$  are easily obtained from the diagonalization of the fine-structure Hamiltonian expressed in the  $m_L, m_S$  representation. For  $H=0$ , they are just the Clebsch-Gordan coefficients for the coupling of a spin of 1 and  $\frac{1}{2}$ . Following the phase convention of Condon and Shortley,<sup>25</sup> we have:

$$\begin{aligned} \mu_0 H = 0: \quad A &= (2/3)^{1/2}, \quad C = (1/3)^{1/2}, \\ &B = (1/3)^{1/2}, \quad D = (2/3)^{1/2}; \\ \mu_0 H = 4\delta W_0/9: \quad (\text{low-field crossing}): \\ A &= (9/11)^{1/2}, \quad C = 6/[73 - (73)^{1/2}]^{1/2}, \\ B &= (2/11)^{1/2}, \quad D = [37 - (73)^{1/2}]^{1/2}/[73 - (73)^{1/2}]^{1/2}; \\ \mu_0 H = 2\delta W_0/3: \quad (\text{high-field crossing}): \\ A &= 2/[\sqrt{17 - 3(17)^{1/2}}]^{1/2}, \quad C = (2/3)^{1/2}, \\ B &= [13 - 3(17)^{1/2}]^{1/2}/[\sqrt{17 - 3(17)^{1/2}}]^{1/2}, \quad D = (1/3)^{1/2}. \end{aligned}$$

The diagonal matrix elements of  $\mathcal{H}_D$  are

$$\begin{aligned} \langle \frac{3}{2}, \frac{3}{2}, m_I | \mathcal{H}_D | \frac{3}{2}, \frac{3}{2}, m_I \rangle &= m_I [(4/5)\alpha\langle 1/r^3 \rangle + \xi/2], \\ \langle \frac{3}{2}, \frac{1}{2}, m_I | \mathcal{H}_D | \frac{3}{2}, \frac{1}{2}, m_I \rangle &= m_I [(2A^2 + 6B^2 - 3\sqrt{2}AB) \\ &\quad \times (\alpha/5)\langle 1/r^3 \rangle + (A^2 - B^2)\xi/2], \\ \langle \frac{3}{2}, -\frac{1}{2}, m_I | \mathcal{H}_D | \frac{3}{2}, -\frac{1}{2}, m_I \rangle &= m_I [(-6C^2 - 2D^2 + 3\sqrt{2}CD) \\ &\quad \times (\alpha/5)\langle 1/r^3 \rangle + (C^2 - D^2)\xi/2], \\ \langle \frac{3}{2}, -\frac{3}{2}, m_I | \mathcal{H}_D | \frac{3}{2}, -\frac{3}{2}, m_I \rangle &= -m_I [(4/5)\alpha\langle 1/r^3 \rangle + \xi/2], \\ \langle \frac{1}{2}, \frac{1}{2}, m_I | \mathcal{H}_D | \frac{1}{2}, \frac{1}{2}, m_I \rangle &= m_I [(2B^2 + 6A^2 + 3\sqrt{2}AB) \\ &\quad \times (\alpha/5)\langle 1/r^3 \rangle + (B^2 - A^2)\xi/2], \\ \langle \frac{1}{2}, -\frac{1}{2}, m_I | \mathcal{H}_D | \frac{1}{2}, -\frac{1}{2}, m_I \rangle &= m_I [(-6D^2 - 2C^2 - 3\sqrt{2}CD) \\ &\quad \times (\alpha/5)\langle 1/r^3 \rangle + (D^2 - C^2)\xi/2]. \end{aligned}$$

<sup>23</sup> R. C. Isler, S. Marcus, and R. Novick, *Bull. Am. Phys. Soc.* **11**, 62 (1966).

<sup>24</sup> R. Novick (private communication).

<sup>25</sup> E. U. Condon and G. H. Shortley, *Theory of Atomic Spectra* (Cambridge University Press, Cambridge, England, 1953).

The off-diagonal matrix elements of interest are those which couple the  $|\frac{3}{2}, -\frac{3}{2}, m_I\rangle$ ,  $|\frac{1}{2}, \frac{1}{2}, m_I\rangle$ , and  $|\frac{1}{2}, -\frac{1}{2}, m_I\rangle$  states to one another and to the rest of the Zeeman states of the  $^2P$  term. They are

$$\begin{aligned} \langle \frac{3}{2}, -\frac{3}{2}, m_I+1 | \mathcal{H}_D | \frac{3}{2}, -\frac{3}{2}, m_I \rangle &= \frac{1}{2} [(I-m_I)(I+m_I+1)]^{1/2} \\ &\quad \times [ (7\sqrt{2}D+2C)(\alpha/10)\langle 1/r^3 \rangle + C\xi ], \\ \langle \frac{3}{2}, -\frac{3}{2}, m_I+1 | \mathcal{H}_D | \frac{1}{2}, -\frac{1}{2}, m_I \rangle &= \frac{1}{2} [(I-m_I)(I+m_I+1)]^{1/2} \\ &\quad \times [ (7\sqrt{2}C-2D)(\alpha/10)\langle 1/r^3 \rangle - D\xi ], \\ \langle \frac{1}{2}, \frac{1}{2}, m_I | \mathcal{H}_D | \frac{3}{2}, \frac{3}{2}, m_I \rangle &= m_I [ (-3\sqrt{2}A^2+3\sqrt{2}B^2+8AB)(\alpha/10)\langle 1/r^3 \rangle - AB\xi ], \\ \langle \frac{1}{2}, \frac{1}{2}, m_I+1 | \mathcal{H}_D | \frac{3}{2}, \frac{3}{2}, m_I \rangle &= \frac{1}{2} [(I-m_I)(I+m_I+1)]^{1/2} \\ &\quad \times [ (-7\sqrt{2}B+2A)(\alpha/10)\langle 1/r^3 \rangle + A\xi ], \\ \langle \frac{1}{2}, \frac{1}{2}, m_I-1 | \mathcal{H}_D | \frac{3}{2}, -\frac{3}{2}, m_I \rangle &= \frac{1}{2} [(I+m_I)(I-m_I+1)]^{1/2} \\ &\quad \times [ (-13\sqrt{2}BC+13\sqrt{2}AD+4BD-12AC) \\ &\quad \times (\alpha/10)\langle 1/r^3 \rangle - BD\xi ], \\ \langle \frac{1}{2}, \frac{1}{2}, m_I-1 | \mathcal{H}_D | \frac{1}{2}, -\frac{1}{2}, m_I \rangle &= \frac{1}{2} [(I+m_I)(I-m_I+1)]^{1/2} \\ &\quad \times [ (13\sqrt{2}BD+13\sqrt{2}AC+4BC+12AD) \\ &\quad \times (\alpha/10)\langle 1/r^3 \rangle - BC\xi ], \\ \langle \frac{1}{2}, -\frac{1}{2}, m_I+1 | \mathcal{H}_D | \frac{3}{2}, \frac{1}{2}, m_I \rangle &= \frac{1}{2} [(I-m_I)(I+m_I+1)]^{1/2} \\ &\quad \times [ (-13\sqrt{2}AD+13\sqrt{2}BC-4AC+12BD) \\ &\quad \times (\alpha/10)\langle 1/r^3 \rangle + AC\xi ], \\ \langle \frac{1}{2}, -\frac{1}{2}, m_I | \mathcal{H}_D | \frac{3}{2}, -\frac{3}{2}, m_I \rangle &= m_I [ (3\sqrt{2}C^2-3\sqrt{2}D^2+8CD) \\ &\quad \times (\alpha/10)\langle 1/r^3 \rangle - CD\xi ]. \end{aligned}$$

#### APPENDIX B: ELECTRIC QUADRUPOLE MATRIX ELEMENTS

Cohen and Reif<sup>26</sup> give general expressions for the matrix elements of the quadrupole Hamiltonian  $\mathcal{H}_Q$  in a form where they can be readily evaluated using the wavefunctions of Appendix A. We will need only the diagonal matrix elements of  $\mathcal{H}_Q$ . Using the formulas on pages 332 and 392 of Ref. 26, we obtain

$$\langle m_I | \mathcal{H}_Q | m_I \rangle = -e^2 Q \frac{[3m_I^2 - I(I+1)]}{4I(2I-1)} \left\langle \frac{3 \cos^2\theta - 1}{r^3} \right\rangle,$$

where  $r$  and  $\theta$  are coordinates of the  $p$  electron cloud. The  $1s$  core electrons do not contribute to the quadrupole interaction. For the two fine-structure levels involved in the low-field crossing

$$\begin{aligned} \langle \frac{3}{2}, -\frac{3}{2}, m_I | \mathcal{H}_Q | \frac{3}{2}, -\frac{3}{2}, m_I \rangle &= b \frac{[3m_I^2 - I(I+1)]}{4I(2I-1)}, \\ \langle \frac{1}{2}, \frac{1}{2}, m_I | \mathcal{H}_Q | \frac{1}{2}, \frac{1}{2}, m_I \rangle &= b \frac{(A^2 - 2B^2)[3m_I^2 - I(I+1)]}{4I(2I-1)}, \end{aligned}$$

where  $b = (2/5)e^2 Q \langle 1/r^3 \rangle$  is the quadrupole interaction constant for the  $^2P_{3/2}$  state defined in the usual manner,<sup>27</sup>

<sup>26</sup> M. H. Cohen and F. Reif, in *Solid State Physics*, edited by F. Seitz and D. Turnbull (Academic Press Inc., New York, 1957), Vol. 5.

<sup>27</sup> H. Kopferman, *Nuclear Moments* (Academic Press Inc., New York, 1958).

and  $A$  and  $B$  are coefficients of the transformation from the  $m_L, m_S, m_I$  to the  $J, m_J, m_I$  representations (see Appendix A). For  $H=0$ , the factor  $A^2-2B^2=0$  and the quadrupole interaction vanishes for the  $|\frac{1}{2}, \frac{1}{2}, m_I\rangle$  states. This agrees with the well-known absence of any quadrupole contribution to the zero-field hyperfine splitting of the  $^2P_{1/2}$  state. At the low-field crossing,  $A^2-2B^2=5/11$ .

#### APPENDIX C: CORRECTION PROCEDURES

##### 1. For Lineshape Asymmetry

The level-crossing signal given by Eq. (7) is of the form

$$S = A(\alpha + \omega)/(1 + \omega^2),$$

where  $\omega$  is the dimensionless ratio  $\Delta/\gamma$ ,  $A$  is nearly a constant, and the value of  $\alpha$  determines the line shape. For  $\alpha \gg 1$  the signal has a Lorentzian lineshape and for  $\alpha = 0$  a dispersion-type line shape. If  $A$  varies linearly over the region of the crossing, we can write  $A = A_0(1 + \beta\omega)$  and  $S$  can be put into the form:

$$S = S_0 + A'(\epsilon + \omega)/(1 + \omega^2), \quad (8)$$

where  $S_0 = A_0\beta$ ,  $A' = A_0(1 + \alpha\beta)$ , and  $\epsilon = (\alpha - \beta)/(1 + \alpha\beta)$ . Thus, except for introducing a small change in the background signal, a variation of  $A$  over the crossing produces to first order the same type of distortion of a Lorentzian signal as does the admixture of a small dispersion-type signal and vice versa.

Lurio and Novick<sup>28</sup> have analyzed in detail the derivative lineshape of a signal having the form of Eq. (8). They show that for a Lorentzian signal ( $\epsilon \gg 1$ ) the derivative peaks occur at approximately  $\omega = \pm 1/\sqrt{3} + 4/9\epsilon$  and the central zero of the derivative signal is shifted by an amount  $1/2\epsilon$ . If the first of these results is used in the derivative of Eq. (8), one obtains  $\Delta/\Sigma = 1/\sqrt{3}\epsilon$ , where  $\Delta$  is the difference in the magnitudes of the two derivative peaks and  $\Sigma$  is the sum of the magnitudes of these peaks. To correct the position of the central zero of the derivative signal, one shifts it toward the *larger* derivative peak by an amount  $\delta\omega = 1/2\epsilon = (\sqrt{3}/2)(\Delta/\Sigma)$ .

The above analysis is adequate for the correction of the low-field crossing signal in  $\text{Li}^7$ , where there is only a slight overlap of the signals from the individual hyperfine crossings, but not for the low-field signal in  $\text{Li}^6$  where there is a large overlap. For  $\text{Li}^6$ , we replace the second term on the right-hand side of Eq. (8) with the sum of three signals whose spacings can be calculated from the spacings in  $\text{Li}^7$  and the known ratio  $g_I(\text{Li}^6)/g_I(\text{Li}^7)$ . The derivative of this expression is then used to relate  $1/\epsilon$  to  $\Delta/\Sigma$  of the outer derivative peaks using the *experimentally observed* spacing of these peaks to calculate  $\Delta$  and  $\Sigma$  as functions of  $1/\epsilon$ . This procedure yields for the correction to the central zero of the derivative signals  $\delta\omega \approx \sqrt{3}(\Delta/\Sigma)$ , where again the meas-

<sup>28</sup> A. Lurio and R. Novick, *Phys. Rev.* **134**, A608 (1964).

ured position should be shifted by this amount toward the larger of the two outer derivative peaks.

Figure 9 of Ref. 28 shows that for a dispersion-type crossing signal ( $\epsilon \ll 1$ ) the two outer derivative peaks are shifted from their positions for  $\epsilon=0$  by an amount  $-\epsilon$ , while the central derivative peak is shifted by  $-\frac{1}{3}\epsilon$ . Differentiation of Eq. (8) shows that the zero-derivative points of a dispersion-type crossing are also shifted (to first order in  $\epsilon$ ) by an amount  $-\epsilon$ . When derivative detection is used, the zero-derivative points can be determined much more precisely (provided a good baseline can be established) than can the positions of the outer derivative peaks. The central derivative peak position is corrected by shifting it *away* from the mean position of the two zero-derivative points by an amount equal to one half the difference between this mean and the observed central peak position.

## 2. For Overlap

The overlap of the signals from the different hyperfine crossings does not shift the position of  $H_0$ , the center

of the  $\text{Li}^6$  low-field crossing signal, but does shift the positions of  $H_1$  through  $H_4$ , the zeros in the derivative of the  $\text{Li}^7$  low-field crossing signal. The resolution of the hyperfine signals in  $\text{Li}^7$  is large enough to allow us to calculate the correction for overlap by considering only two hyperfine signals at a time and then adding the results for all such overlapping pairs. For two overlapping Lorentzian signals, the signal is proportional to  $[1+(\omega-\omega_0)^2]^{-1} + [1+(\omega+\omega_0)^2]^{-1}$ , where again  $\omega$  is the dimensionless ratio  $\Delta/\gamma$  and  $2\omega_0$  is the dimensionless spacing of the two hyperfine crossings. Setting the derivative of this expression equal to zero yields, in addition to the obvious root at  $\omega=0$ ,

$$\omega^2 = 2\omega_0(\omega_0^2 + 1)^{1/2} - (\omega_0^2 + 1).$$

The differences between the roots of this equation and  $\omega = \pm\omega_0$  give the shifts of the derivative zeros arising from the overlap. If  $\omega_0^2 < \frac{1}{3}$ , the equation has no real roots and the only zero in the derivative signal is the one at  $\omega=0$ . For the  $\text{Li}^7$  low-field signal, the spacings of adjacent hyperfine crossings correspond to an  $\omega_0$  of very nearly 2.

## “Anticrossing” Signals in Resonance Fluorescence\*

H. WIEDER† AND T. G. ECK

*Physics Department, Case Institute of Technology, Cleveland, Ohio*

(Received 26 August 1966)

The level-crossing technique of atomic spectroscopy utilizes the spatial interference in the scattering of resonance radiation which can occur when two Zeeman levels of an atom are brought into coincidence (“crossed”) by the application of an external magnetic field. “Anticrossing” refers to the case where the two levels involved are coupled by a small static interaction. In this paper the general expression for an anticrossing signal is given and its predictions compared with signals observed in the  $2^2P$  term of Li. It is shown that anticrossings produce signals in many experimental situations for which there would be no signal from a normal level crossing.

### I. INTRODUCTION

THE two most widely used techniques for investigating the fine and hyperfine structure of excited states of atoms are those of optical-double-resonance (ODR)<sup>1</sup> and level-crossing.<sup>2</sup> In both of these techniques, signals are seen which are the result of a “coupling” between two Zeeman levels of the excited state. For ODR experiments, this coupling is accomplished by the application of a rf magnetic field having the appropriate frequency, while for a level crossing the coupling in the region of the crossing is simply an intimate part of the

optical excitation process.<sup>3</sup> In this paper we consider the situation where two crossing levels are coupled by a small static interaction (as opposed to the time-dependent coupling of ODR). The static interaction can give rise to a signal even if the properties of the optical excitation or of the two levels are such as to prohibit the presence of a normal level-crossing signal. The word “anticrossing”<sup>4,5</sup> has been used to distinguish this case from a normal level crossing, because it is descriptive of the manner in which the coupled levels “repel” one another as the magnetic field is varied through the region of close approach. We discuss anticrossing signals that we have observed in the  $2^2P$  term of Li and

\* Work supported by the National Science Foundation.

† Present address: IBM T. J. Watson Research Center, Yorktown Heights, New York.

<sup>1</sup> J. Brossel and F. Bitter, *Phys. Rev.* **86**, 308 (1952).

<sup>2</sup> F. D. Colegrove, P. A. Franken, R. R. Lewis, and R. H. Sands, *Phys. Rev. Letters* **3**, 420 (1959).

<sup>3</sup> P. A. Franken, *Phys. Rev.* **121**, 508 (1961).

<sup>4</sup> T. G. Eck, L. L. Foldy, and H. Wieder, *Phys. Rev. Letters* **10**, 239 (1963).

<sup>5</sup> T. G. Eck, paper presented at the Zeeman Centennial conference (to be published).